scriptional regulators. Although a function extrinsic to TFIID cannot be excluded, the co-fractionation of all detectable p250/CCG1 with TFIID (data not shown) argues that it subserves a major cell cycle function as part of TFIID.

Only some G1 transcription functions are disrupted in ts cell mutants that can be complemented by wild-type p250/CCG1 (ts13 and tsBN462), and the cells survive for some time at the restrictive temperature[18,19,30]. The transcription defect in these cells thus appears to be restricted to only some genes, possibly those controlled by transcription factors with a particular type of activation domain. Such a domain might interact with a region of p250/CCG1 not otherwise used as an activator target (perhaps modified at certain stages of the cell cycle), so affording an additional checkpoint for cell cycle progression. □

Received 11 February; accepted 18 February 1993.

1. Matsui, T., Segall, J., Weil, P. A. & Roeder, R. G. *J. biol. Chem.* **255,** 11992-11996 (1980).
2. Van Dyke, M. W., Roeder, R. G. & Sawadogo, M. *Science* **241,** 1335-1338 (1988).
3. Horikoshi, M., Hai, T., Lin, Y.-S., Green, M. R. & Roeder, R. G. *Cell* **54,** 1033-1042 (1988).
4. Buratowski, S., Hahn, S., Guarente, L. & Sharp, P. A. *Cell* **56,** 549-561 (1989).
5. Sawadogo, M. & Roeder, R. G. *Cell* **43,** 165-175 (1985).
6. Nakajima, N., Horikoshi, M. & Roeder, R. G. *Molec. cell. Biol.* **8,** 4028-4040 (1988).
7. Dynlacht, B. D., Hoey, T. & Tjian, R. *Cell* **66,** 563-576 (1991).
8. Tanese, N., Pugh, B. F. & Tjian, R. *Genes Dev.* **5,** 2212-2224 (1991).
9. Takada, R. *et al. Proc. natn. Acad. Sci. U.S.A.* **89,** 11809-11813 (1992).
10. Zhou, Q., Lieberman, P., M., Boyer, T. G. & Berk, A. *Genes Dev.* **6,** 1964-1974 (1992).
11. Hoffmann, A. *et al. Nature* **346,** 387-390 (1990).
12. Peterson, M. G., Tanese, N., Pugh, B. F. & Tjian, R. *Science* **248,** 1625-1630 (1990).
13. Stringer, K. F., Ingles C. J. & Greenblatt, J. *Nature* **345,** 783-786 (1990).
14. Lee, W. S., Kao, C. C., Bryant, G. O., Liu, X. & Berk, A. J. *Cell* **67,** 365-376 (1991).
15. Lin, Y.-S. & Green, M. R. *Cell* **64,** 971-981 (1991).
16. Horikoshi, M., Carey, M. F., Kakidani, H. & Roeder, R. G. *Cell* **54,** 665-669 (1988).
17. Workman, J. M., Abmayr, S. M., Cromlish, W. A. & Roeder, R. G. *Cell* **55,** 211-219 (1988).
18. Sekiguchi, T., Miyata, T. & Nishimoto, T. *EMBO J.* **7,** 1683-1687 (1988).
19. Sekiguchi, T., Nohiro, Y., Nakamura, Y., Hisamoto, N. & Nishimoto, T. *Molec. cell. Biol.* **11,** 3317-3325 (1991).
20. Nikolov, D. B. *et al. Nature* **360,** 40-46 (1992).
21. Malik, S., Hisatake, K., Sumimoto, H., Horikoshi, M. & Roeder, R. G. *Proc. natn. Acad. Sci. U.S.A.* **88,** 9553-9557 (1991).
22. Tamkun, J. W. *et al. Cell* **68,** 561-572 (1992).
23. Haynes, S. R., Dollard, C., Winston, F., Beck, S. & Dawid, I. *Nucleic Acids Res.* **20,** 2603 (1992).
24. Georgakopoulos, T. & Thireos, G. *EMBO J.* **11,** 4145-4152 (1992).
25. Bianchi, M. E., Falciola, L., Ferrari, S. & Lilley, D. M. J. *EMBO J.* **11,** 1055-1063 (1992).
26. Ferrari, S. *et al. EMBO J.* **11,** 4497-4506 (1992).
27. Helman, J. D. & Chamberlin, M. J. *A. Rev. Biochem.* **57,** 839-872 (1988).
28. Johnston, L. H. *Trends Cell Biol.* **2,** 353-357 (1992).
29. Schmid, R. M., Perkins, N. D., Duckett, C. S., Andrews, P. C. & Nabel, G. J. *Nature* **352,** 733-736 (1991).
30. Liu *et al. J. biol. Chem.* **260,** 3269-3274 (1985).

ACKNOWLEDGEMENTS. We thank T. Kokubo for preparing oligonucleotides, and T. Morinaga, R. Kageyama and S. Nakanishi for human cDNA libraries. Protein sequencing was done by the Protein Sequence Facility of The Rockefeller University. K.H. is supported by a fellowship from Toyobo Biotechnology Foundation. R.T. was supported by a fellowship from the Uehara Memorial Foundation. M.H. was an Alexandrine and Alexander L. Sinsheimer Scholar. A part of this research was supported by grants from Nippon Suisan Kaisha Ltd (to Y.N.), Special Project Research from the Ministry of Education, Science and Culture of Japan (to M.H.) and the National Institutes of Health (to R.G.R. and M.H.) and by general support from the Pew Trusts to The Rockefeller University.

Yeast $tRNA^{Asp}$ recognition by its cognate class II aminoacyl-tRNA synthetase

Jean Cavarelli, Bernard Rees, Marc Ruff, Jean-Claude Thierry & Dino Moras*

Laboratoire de Biologie Structurale, IBMC Strasbourg-Cedex, France

AMINOACYL-RNA synthetases can be divided into two classes according to structural features inferred from sequence alignments[1–3]. This classification correlates almost perfectly with the attachment of the amino acid to the 2′-OH (class I) or 3′-OH (class II) group of the terminal adenosine[4–6]. Six subgroups of higher homology can be inferred from sequence analysis[7,8]. The five aminoacyl-tRNA synthetases whose crystal structures are known (MetRS, TyrRS and GlnRS in class I, SerRS and AspRS in class II)[9–13] belong to different subgroups. Two of them, GlnRS and AspRS, have been cocrystallized with their cognate tRNA[11,13]. AspRS, like six other members of class II, is an α_2 dimer. Yeast $tRNA^{Asp}$ exhibits five identity determinants: the three anticodon bases, the discriminator base G73 and the base pair G10–U25[14]. We report here that the refined crystal structure of AspRS complexed with $tRNA^{Asp}$ at 2.9 Å resolution reveals three regions of contact, each involving a domain of AspRS and at least one identity determinant of $tRNA^{Asp}$. The mode of binding of the acceptor stem of $tRNA^{Asp}$ by AspRS can be generalized to class II aminoacyl-tRNA synthetases, whereas the deciphering of the anticodon, which involves a large conformational change of the loop and the formation of a bulge, is more specific to the aspartic system.

Although the aspartyl-tRNA synthetase (AspRS) dimer has a rather compact shape, each subunit is very elongated and shows two distinct domains connected by a small hinge module (Fig. 1). The C-terminal domain (residues 241–557) is the largest and contains the active site. The three conserved motifs of class II synthetases are found in this region[1]. The N-terminal domain is involved in the recognition of the anticodon of the tRNA. The dimeric enzyme binds two tRNA molecules symmetrically but with some differences at the active site (Table 1). Apart for one interaction between Lys 293, which is part of the first conserved motif, and the phosphate group of U1, all direct contacts formed by one tRNA molecule involve the same synthetase monomer (Table 1). The total buried surface or contact area of one tRNA molecule is 2,500 $Å^2$. This represents about 20% of the solvent-accessible surface of the free tRNA and is similar to what was observed in the glutaminyl system[11]. The N-terminal domain makes few interactions with the C-terminal domain of the same monomer but forms an important interface with the C-terminal domain of the other subunit. Thus, information may be transferred in a cooperative manner from the N-terminal domain of one subunit to the active site of the other subunit.

The main feature of the C-terminal domain is the active-site cavity formed by a six-stranded antiparallel β-sheet and partly closed by loops and α-helices[13]. This region contains the three signature motifs of class II aminoacyl-tRNA synthetases (aaRS), which interact with the acceptor stem of the tRNA and perform the catalysis (Fig. 2*a*). Motifs 1 and 2 participate in the positioning of the acceptor stem and motif 2 and 3 bind the ATP. This suggests that the mechanism involved in the recognition of this part of the tRNA can probably be generalized to most if not all class II synthetases. Two loops clamp the acceptor stem of the tRNA. The variable loop of motif 2 (residues 327–334) approaches the tRNA molecule on the major groove side and interacts with the discriminator base G73 and the first base pair of the stem. Another segment (residues 423–428) interacts with the phosphate groups of A72 and G73. This peptide is part of a domain (residues 373–438) of variable size within the aaRS inserted after motif 2.

The hinge connecting the C-terminal and N-terminal domains of the protein is a distinct globular module of four short helices (residues 207–240). It interacts with the ribose and phosphate groups of U11 and U12 rather than with the determinant G10–U25 (Fig. 2*b* and table 1). The molecular mechanism by which the determinant acts is not protein-mediated: mutations of G10 or U25 are likely to disrupt the tertiary interaction formed with G45 and thus lead to a conformational change in this part of

* To whom correspondence should be addressed.

the tRNA. This agrees with the observation that such mutations affect the Michaelis constant, K_M, in contrast with mutations at other determinants, which affect the catalysis constant K_{cat} (ref. 14).

The N-terminal domain is built around a five-stranded β-barrel. The domain approaches the anticodon loop of the tRNA on the side of the major groove (Fig. 3*a*). If the strands are numbered in the order of the sequence, the topological succession is S1 S4 S5 S3 S2 S1. Successive strands are antiparallel, except S5 and S3. An α-helix is inserted between strands S3 and S4. The same topological organization has been found in completely different enzymes, namely staphylococcal nuclease[15], heat-labile enterotoxin[16] and verotoxin-1[17] (A. Murzin, personal communication). In all these enzymes, this region is involved in the binding of either nucleotides or oligosaccharides. The interaction with the anticodon loop is specific to the AspRS system, but sequence analyses have shown that the principles can probably be generalized to the subgroup comprising AspRS, AsnRS and LysRS[18–20]. Because no significant homology with other aaRS could be detected, the N-terminal domain may be characteristic of the subgroup specificity. In this domain, 5 of the 14 amino acids involved in direct contacts with tRNA are conserved both in prokaryotic and eukaryotic AspRS, and in the subgroup of AspRS, AsnRS and LysRS from *Escherichia coli*. Three of the residues (Phe 127, Gln 138 and Arg 119) recognize the base U35 which is conserved in the cognate tRNAs of the members of the subgroup. Arg 119 also interacts with the ribose of residue C36. The fourth, Glu 188, which in the yeast AspRS system binds G34, can interact equally well with the modified guanine present in the $tRNA^{Asp}$ and $tRNA^{Asn}$ from different organisms. In $tRNA^{Lys}$, the nucleotide in position 34 is cytidine, uridine or one of their derivatives. Note that Lys 142, which also binds G34 of yeast $tRNA^{Asp}$, is not present in *E. coli* to make space for the bulky base Q (queuosine). The fifth conserved residue, Gly 122, plays a pivotal role at the end of the β-sheet where any side chain would interfere with the base at position 32 in the anticodon stem.

The three bases of the anticodon are protruding out to maximize contacts with the protein, which illustrates the flexibility of the tRNA molecule (Fig. 3*b*). When compared to the situation in the free state[21,22], the conformation of $tRNA^{Asp}$ in the complex is characterized by the closing of the two limbs. The regular RNA A-form double helix of the acceptor stem is not altered, but the anticodon stem is smoothly bent inward starting with base pair G27–C43. The most striking feature is that the anticodon loop (bases ψ32 to C38) has unravelled so that five bases protrude outward. The backbone forms a bulge at the modified purine 37 (m1G37) which is stabilized by two intramolecular hydrogen bonds, one between the O2′ of C38 and the phosphate of C36, and the other between the N2 of m1G37 and the phosphate of U25.

The crystal structure of yeast $tRNA^{Asp}$–AspRS complex confirms the modular character of the members of the synthetase family and clarifies the role of each structural component. The manner in which the active site domain binds the CCA end of $tRNA^{Asp}$ and ATP can probably be considered a model of class

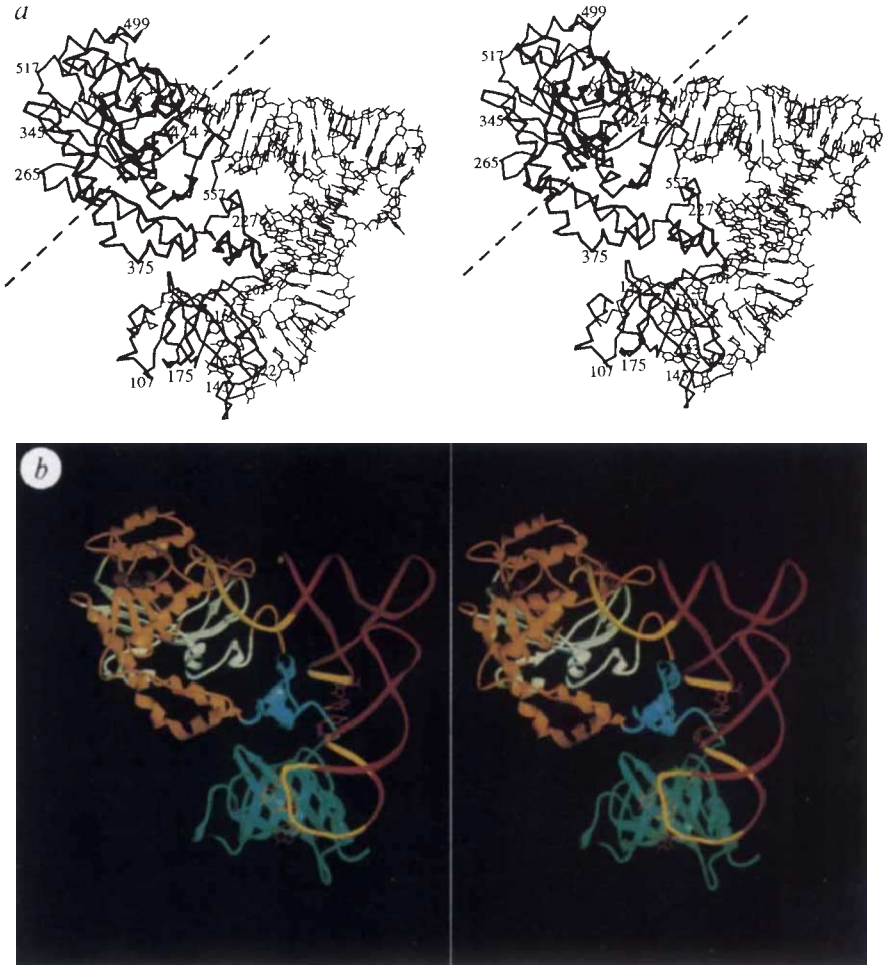

FIG. 1 *a*, General view of the complex. One monomer of AspRS (Cα backbone) and one molecule of $tRNA^{Asp}$ are shown. The position of the local twofold axis is indicated. This and the other black-and-white stereopictures were made using the program MOLSCRIPT[25]. The first 65 residues of each monomer of AspRS are at least partly disordered in the crystal and could not be traced in the maps. They are not essential because it has been shown that the first 75 residues can be removed by mild digestion without affecting the enzymatic activity of the protein[26]. Crystals belong to space group $P2_12_12$ with unit cell parameters $a=210.2$ Å, $b=146.2$ Å, $c=86.1$ Å and with one dimeric molecule per asymmetric unit. The crystal structure was solved by multiple isomorphous replacement with three derivatives and the phases were improved by solvent flattening and noncrystallographic symmetry averaging. The model was refined through energy minimization with X-PLOR[27]. The *R*-factor is 23.1% for 49,370 reflections (90% of possible data, $F/\text{sig}(F)>3$) in the 7–2.9 Å resolution range without including any solvent molecules. The r.m.s. bond deviation from ideality is 0.010 Å and r.m.s. angle deviation is 1.8°. The mean *B*-factor is 30 Å^2. *b*, Regions of interaction between AspRS and $tRNA^{Asp}$ (program RIBBONS[28]). The contact regions of the tRNA are in yellow, with the identity determinants shown. The C-terminal domain of AspRS is in brown, with class II signature motifs in white. The N-terminal domain is in green and the junction peptide in blue.

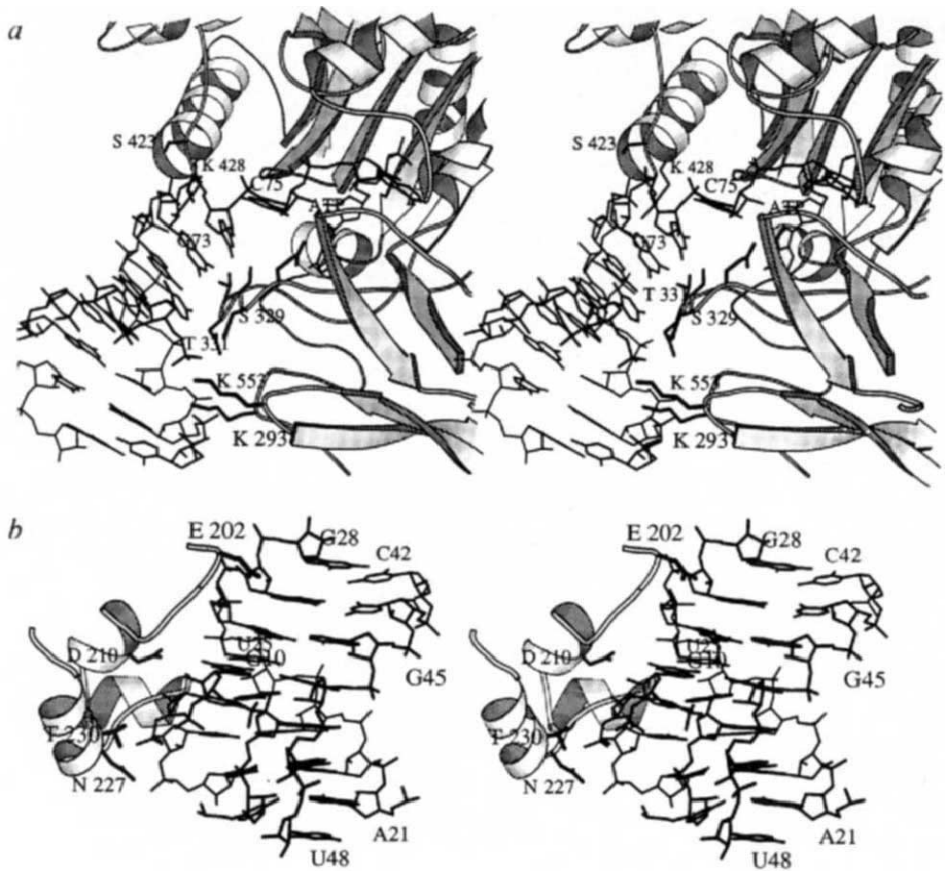

FIG. 2 *a*, Contacts in the region of the acceptor stem of $tRNA^{Asp}$. Residues 327–331, which form the variable part of the second conserved motif of class II synthetases, make base-specific hydrogen bonds with the discriminator base G73 and the first base pair U1–A72. Ser 423, Thr 424 and Lys 428 bind to the phosphate groups of A72 and G73. The phosphate group of U1 is responsible for the only interaction with the other synthetase monomer, through Lys 293. *b*, Contacts in the region of the D-stem of $tRNA^{Asp}$. The ribose-phosphate backbone from U11 to U12 is secured by a number of interactions with protein residues Glu 202, Asp 210, Asn 227 and Thr 230. This is the region forming the hinge between the C-terminal and the N-terminal domains. None of these interactions is base-specific, and none involves the determinant base pair G10–U25.

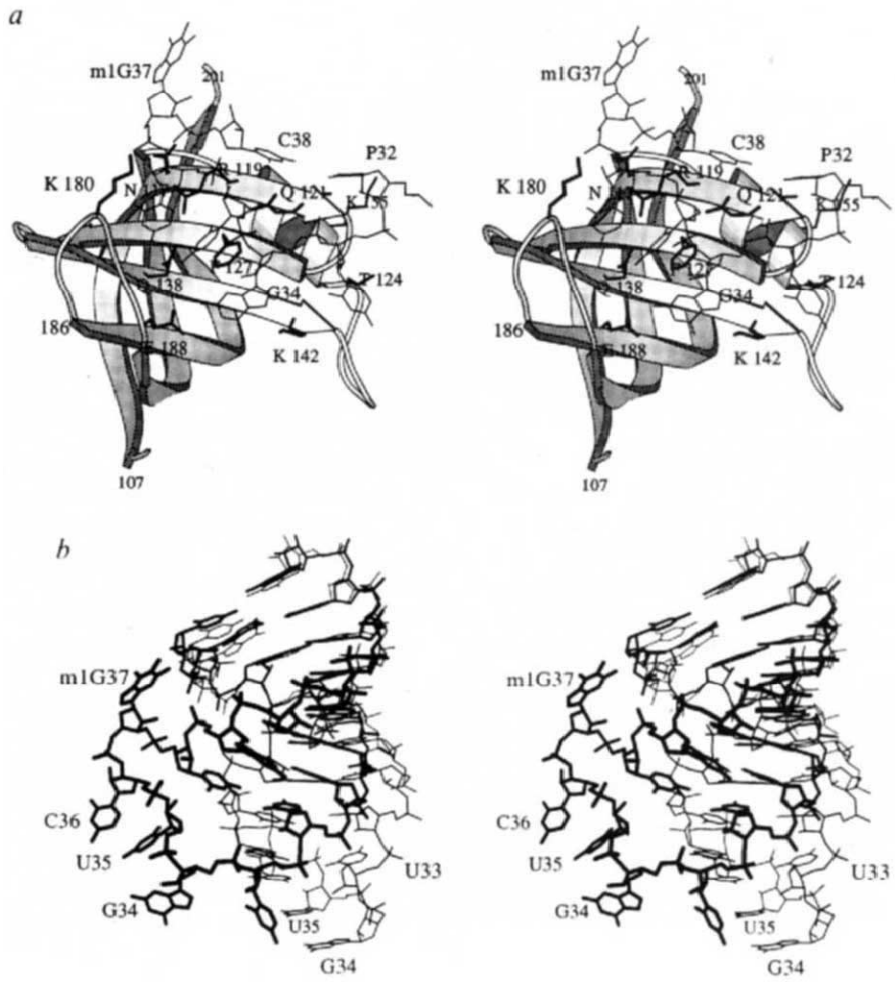

FIG. 3 *a*, Contacts in the region of the anticodon of $tRNA^{Asp}$. Lys 155, a strictly conserved residue in all known AspRS, binds to the phosphate groups of G30, an interaction which may be important for the correct relative positioning of the protein and the anticodon stem. The guanine G34 forms two hydrogen bonds with the conserved Glu 188 and interacts with Lys 142 through N7, in agreement with protection experiments toward dimethylsulphate done in solution[29]. U35 is sandwiched between C36 and the strictly conserved Phe 127, and forms a hydrogen bond with the conserved Gln 138. C36 is hydrogen bonded to main chain groups of Pro 178 and Lys 180; its ribose binds to the side chain of the conserved Arg 119. *b*, Superposition of the anticodon stem and loop in the free (thin line) and complexed (thick line) $tRNA^{Asp}$. In the complex, the canonical U-turn conformation is disrupted after Ψ32. Ψ32 and C38 form an additional distorted non-Watson–Crick base pair (one hydrogen bond between Ψ32 O4 and C38 N4) stacked over C31–G39. U33 points toward the solvent with a weak connection to the enzyme. The stacking of the anticodon bases observed in free $tRNA^{Asp}$ is totally unravelled. G34 makes no contact with U35 which is imperfectly stacked to C36 while being associated with Phe 127.

TABLE 1 tRNA synthetase interactions (distance <3.5 Å)

tRNA		AspRS	
U1	OP	**Lys 293***	Nζ
	OP	Asn 328	Nδ
	O4	*Asn 330*	N
A72	OP	*Lys 428*	Nζ
	N6	*Asn 330*	O
G73	OP	*Thr 424*	Oγ
	OP	*Ser 423*	Oγ
	O6†	*Thr 331*	Oγ
	N1†	*Ser 329*	Oγ
	N2†	Asn 328	O
	N2†	**Glu 327**	Oε
C74	N3†	*Ser 329*	Oγ
	N4†	*His 334*	Nε
C67	OP	*Lys 553*	Nζ
U11	O2′	*Asp 210*	Oδ
U12	OP	*Thr 230*	Oγ
	OP	**Asn 227**	N
G27	O2′	Glu 202	Oε
G30	OP	**Lys 155**	Nζ
Ψ32	N3	Gln 120	O
U33	O4	Thr 124	Oγ
G34	N7	Lys 142	Nζ
	N2	**Glu 188**	Oε
U35	O4′	Gln 121	Nε
	N3	**Gln 138**	Oε
	O2	**Arg 119**	Nη
	—	**Phe 127**	Stacking
C36	O4′	**Arg 119**	Nη
	O2	*Ser 181*	Oγ
	O2	Lys 180	N
	N4	Pro 178	O
m1G37	OP	Lys 180	Nζ
C38	OP	Asn 117	Nδ
	N4	Gln 120	O
	N3	Gln 121	Oε

Interactions within the active site (nucleotides C75 and A76) are not included. Residues in bold are highly conserved in all AspRS, whereas those in italics are conserved in eukaryotes only. In tRNA, phosphate oxygens are named OP, atoms with primes belong to the ribose, all others to the base.

* This residue belongs to the other subunit.

† The conformations are different in the two subunits. In the map of the binary complex the active sites are different in the two subunits. In subunit B, although the crystals were grown in the absence of ATP in the mother liquor, a clear electron density is visible in which an AMP model can be fitted. In the other subunit, this site is partially occupied by the terminal adenosine of tRNA as a result of a conformational change which extends up to the first base pair of the acceptor stem. In subunit B, where the CCA end of tRNA occupies its functional location, A76 is stacked on Phe 304 with its ribose group above and close to the β phosphate of ATP. The ATP binding site essentially comprises the class II conserved Glu 327 and Phe 338 (stacked on the purine ring) and the glycine-rich strand of motif 3 (Gly 526–Gly 528) which interacts with the ribose-phosphate groups. The invariant residues of motifs 2 and 3 bind to the α-phosphate (Arg 325) and to the ribose (Arg 531). Addition of ATP to the crystals leads to fully symmetrical dimers. A detailed analysis of the structure–function relationship in the active site will be published (J.C. *et al.*, manuscript in preparation).

II aaRS. Subgroup specificity is then obtained by the addition of a module at the N-terminal end. Another module, not conserved in prokaryotic AspRS, is inserted after the conserved motif 2 of class II and plays an important role in the specific recognition of tRNA. An additional recognition element interacting with the minor groove of the acceptor stem may be present in some class II enzymes, for example in the *E. coli* AlaRS system where the main tRNA identity determinant is the third base pair of the acceptor stem[23,24]. The insertion peptide after motif 2 could also act as a minor groove recognition module. □

Received 24 August; accepted 22 December 1992.

1. Eriani, G., Delarue, M., Poch, O., Gangloff, J. & Moras, D. *Nature* **347,** 203–206 (1990).
2. Webster, T., Tsai, H., Kula, M., Mackie, G. A. & Schimmel, P. *Science* **226,** 1315–1317 (1984).
3. Hountondji, C., Dessen, P. & Blanquet, S. *Biochimie* **68,** 1071–1078 (1986).
4. Fraser, T. H. & Rich, A. *Proc. natn. Acad. Sci. U.S.A.* **72,** 3044–3048 (1975).
5. Von der Haar, F. & Cramer, F. *Biochemistry* **15,** 4131–4136, (1976).
6. Hecht, S. M. *Transfer RNA: Structures, Properties and Recognition* (eds P. P. Schimmel, D. Söll & J. N. Abelson) 345–360 (Cold Spring Harbor Laboratory Press, New York, 1979).
7. Cusack, S., Härtlein, M. & Leberman, R. *Nucleic Acids Res.* **19,** 3489–3498 (1991).
8. Moras, D. *Trends biochem. Sci.* **17,** 159–164 (1992).
9. Brick, P., Bhat, T. N. & Blow, D. M. *J. molec. Biol.* **208,** 83–98 (1989).
10. Brunie, S., Zelwer, C. & Risler, J. L. *J. molec. Biol.* **216,** 411–424 (1990).
11. Rould, M. A., Perona, J. J., Söll, D. & Steitz, T. A. *Science* **246,** 1135–1142 (1989).
12. Cusack, S., Berthet-Colominas, C., Härtlein, M., Nassar, N. & Leberman, R. *Nature* **347,** 249–255 (1990).
13. Ruff, M. *et al. Science* **252,** 1682–1689 (1991).
14. Pütz, J., Puglisi, J. D., Florentz, C. & Giegé, R. *Science* **252,** 1696–1699 (1991).
15. Hynes, T. R. & Fox, R. O. *Proteins* **10,** 92–105 (1991).
16. Sixma, T. K. *Nature* **355,** 561–564 (1992).
17. Stein, P. E., Boodhoo, A., Tyrrell, G. J., Brunton, J. L. & Read, R. J. *Nature* **355,** 748–750 (1992).
18. Eriani, G., Dirheimer, G. & Gangloff, J. *Nucleic Acids Res.* **18,** 7109–7117 (1990).
19. Anselme, J. & Hartlein, M. *Gene* **84,** 481–485 (1989).
20. Leveque, F., Plateau, P., Dessen, P. & Blanquet, S. *Nucleic Acids Research* **18,** 305–312 (1990).
21. Moras, D. *et al. Nature* **288,** 669–674 (1980).
22. Westhof, E., Dumas, P. & Moras, D. *J. molec. Biol.* **184,** 119–145 (1985).
23. McClain, W. H. & Foss, K. *Science* **241,** 1804–1807 (1988).
24. Hou, Y. M. & Schimmel, P. *Nature* **333,** 140–145 (1988).
25. Kraulis, P. J. *J. appl. Crystallogr.* **24,** 946–950 (1991).
26. Eriani, G. *et al. Eur. J. Biochem.* **200,** 337–343 (1991).
27. Brünger, A. T. *J. molec. Biol.* **203,** 803–816 (1988).
28. Carson, M. K. *J. appl. Crystallogr.* **24,** 958–961 (1991).
29. Garcia, A. & Giegé, R. *Biochem. biophys. Res. Commun.* **186,** 956–962 (1992).

ACKNOWLEDGEMENTS. We want to express our gratitude to the late J. P. Ebel. His continuous support from the beginning was decisive for the success of the project. We thank M. Boeglin, M. Delarue, A. Mitschler and A. Poterszman for unpublished data on the ternary complex and on the *Thermus thermophilus* AspRS, G. Eriani, J. Gangloff, R. Giégé, D. Kern, J. Pütz and J. Rudinger for discussions and J. Arnez for his comments on the manuscript. This work was supported by grants from the Human Science Frontier Program and the EEC Science Program.

CORRECTION

Lead isotope evidence for young trace element enrichment in the oceanic upper mantle

Alex N. Halliday, Gareth R. Davies, Der-Chuen Lee, Simone Tommasini, Cassi R. Paslick, J. Godfrey Fitton & Dodie E. James

Nature **359,** 623–627 (1992)

WE have been unable to precisely reproduce some of the lead isotope data for Madeira lavas reported in the above paper. In the light of further analyses the correct compositions are as follows:

Sample number	$^{206}Pb/^{204}Pb$	$^{207}Pb/^{204}Pb$	$^{208}Pb/^{204}Pb$
MD4	19.159	15.533	38.825
MD10	19.182	15.535	38.864
MD32	19.097	15.559	38.946
MD40	19.143	15.573	38.864
MD64	19.038	15.556	38.753

The $^{207}Pb/^{204}Pb$, $^{87}Sr/^{86}Sr$ and $^{143}Nd/^{144}Nd$ ratios still plot within the field of Atlantic MORB, whereas the $^{206}Pb/^{204}Pb$ and $^{208}Pb/^{204}Pb$ ratios are relatively high for MORB. Therefore, although the revised Pb isotopic compositions plot closer to other OIB, the overall interpretation is unchanged. □